J. Membrane Biol. 132, 253–265 (1993)

The Journal of
Membrane Biology


# Enzyme Kinetics of the Prime $K^+$ Channel in the Tonoplast of *Chara*: Selectivity and Inhibition

Hans-Georg Klieber*, and Dietrich Gradmann
Pflanzenphysiologisches Institut der Universität, 3400 Göttingen, Germany

**Summary.** The prime potassium channel from the tonoplast of *Chara corallina* has been analyzed in terms of an enzyme kinetic model (Gradmann, Klieber & Hansen 1987, *Biophys. J.* **53**:287) with respect to its selectivity for $K^+$ over $Rb^+$ and to its blockage by $Cs^+$ and by $Ca^{2+}$. The channel was investigated by patch-clamp techniques over a range of membrane voltages ($V_m$, referred to an extracytoplasmic electrical potential of zero) from −200 mV to +200 mV under various ionic conditions (0 to 300 mM $K^+$, $Rb^+$, $Cs^+$, $Ca^{2+}$, and $Cl^-$) on the two sides of isolated patches. The experimental data are apparent steady-state current-voltage relationships under all experimental conditions used and amplitude histograms of the seemingly noisy open-channel currents in the presence of $Cs^+$. The used model for $K^+$ uniport comprises a reaction cycle of one binding site through four states, i.e., (1) $K^+$-loaded and charged, facing the cytoplasm, (2) $K^+$-loaded and charged facing the vacuole, (3) empty, facing the vacuole, and (4) empty, facing the cytoplasm. $V_m$ enters the system in the form of a symmetric Eyring barrier between state 1 and 2. The numerical results for the individual rate constants are (in $10^6 s^{-1}$ for zero voltage and 1 M substrate concentration): $k_{12}$: 1,410, $k_{21}$: 3,370, $k_{23}$: 105,000, $k_{32}$: 10,600, $k_{34}$: 194, $k_{43}$: 270, $k_{41}$: 5,290, $k_{14}$: 15,800. For the additional presence of an alternate transportee (here $Rb^+$), the model can be extended in an analog way by another two states ((5) $Rb^+$-loaded and charged, facing cytoplasm, and (6) $Rb^+$-loaded and charged, facing vacuole) and six more rate constants ($k_{45}$: 300, $k_{54}$: 240, $k_{56}$: 498, $k_{65}$: 4,510, $k_{63}$: 4,070, $k_{36}$: 403). This six-state model with its unique set of fourteen parameters satisfies the complete set of experimental data. If the competing substrate can be bound but not translocated (here $Cs^+$ and $Ca^{2+}$), $k_{56}$ and $k_{65}$ of the model are zero, and the stability constants $K_{cyt}$ (= $k_{36}/k_{63}$) and $K_{vac}$ (= $k_{45}/k_{54}$) turn out to be $K_{cyt}(Ca^{2+})$: 250 $M^{-1} \cdot \exp(V_m/(64\ mV))$, $k_{vac}(Ca^{2+})$: 10 $M^{-1} \cdot \exp(-V_m/(66\ mV))$, $K_{cyt}(Cs^+)$: 0, and $K_{vac}(Cs^+)$: 46 $M^{-2} \cdot \exp(-V_m/(12.25\ mV))$. With the assumption that the current fluctuations in the presence of $Cs^+$ consist of incompletely resolved, short periods of complete openings and complete closures, the amplitude histograms of the noisy open channel currents can be described by a beta distribution, yielding the rate constants for binding ($92 \cdot 10^6\ sec^{-1} \cdot M^{-2} \cdot \exp(-V_m/(22.5\ mV))$ and debinding ($2 \cdot 10^6\ sec^{-1} \cdot M^{-2} \cdot \exp(V_m/(22.5\ mV))$ of $Cs^+$ to the vacuolar side of the channel as functions of the $[Cs^+]$ and of $V_m$. Considering these data and those from the literature, an asymmetry of the channel can be assessed, with a high charge density at the cytoplasmic side (Eisenman-series Nr. XI) and a low charge density at the vacuolar side (Eisenman-series Nr. I). Furthermore, the results provide an example for intimate linkage between conduction and switching of a channel.

**Key Words** *Chara corallina* · enzyme kinetics · gating · open-channel noise analysis · potassium channel · selectivity

## Introduction

Ion channels can be viewed as enzymes in a literal sense, because they are proteins which *catalyze* the transition of ions through lipid membranes. Under this aspect, the electrical conductance of an ion channel can be expected to correspond to enzyme kinetic relationships. This matter has been worked out with various emphases on essentially the same subject (for reviews *see* Cooper, Jakobsson & Wolynes, 1985; Levitt, 1986; or Cooper, Gates & Eisenberg, 1988). Most current models comprise at least two binding sites in series because ion channels are generally accepted to operate in a single-file diffusion mode. The corresponding reaction kinetic schemes have many parameters that usually cannot be determined unambiguously by the experimental data available. Thus, the analysis does not usually result in a unique set of definite parameters but in families of possible solutions. This disadvantage was one reason to reexamine more simple models which may enable the solution of the inverse problem, namely to find a unique set of parameters which satisfies the observations.

The theoretical background of our approach originates from a general concept for ion transport (Läuger, 1980). Details for practical application of the theory have been communicated previously together with a practical example (Gradmann et al.,

* *Present address:* Physiologisches Institut der Technischen Universität, Biedersteinerstr. 29, W-8000 Munich 40, Germany

1987). Subsequent applications of the model to open channel uniport through ion channels from plants and fungi have been successful as well (Fisahn, Hansen & Gradmann 1986; Bertl & Gradmann, 1987; Bertl, 1989; Spalding et al., 1992).

The basic model used here operates with the following assumptions: there is only one binding site, and only one voltage-dependent reaction step (for the translocation of the charged substrate) with a symmetric Eyring barrier. Actually, the experimental data require an extension of the simplest three-state model (Fig. 1*A*) to a four-state model by an extra reaction step for the reorientation of the unoccupied binding site (Fig. 1*B*). If more than one substrate is considered, additional reactions have to be introduced, e.g., the reaction scheme of Fig. 1*C* can be used for competitive translocation of $K^+$ and $Rb^+$, or for blockage by $Cs^+$ or by $Ca^{2+}$. This study demonstrates that this approach is appropriate for the competitive translocation of two different ion species by an individual channel and for competitive blocking.

Crucial for this treatment are channel currents which saturate at large voltage displacements from equilibrium due to the limited turnover of the channel itself and not to the limited diffusion from the bulk solution to the binding site. Such channels are frequently found in plant membranes (*cf.* Schroeder, Hedrich & Fernandez, 1984; Lühring, 1986; Bertl & Gradmann, 1987) where they can be investigated over a wide voltage range.

The system used here is the prime $K^+$ channel in the tonoplast of *Chara corallina*. The initial suggestion that this channel originates from the tonoplast (Lühring, 1986) has been confirmed by its identification in the membrane of isolated vacuoles (Bertl, 1989). Thus, the data provided here from a well-defined channel could be obtained again by more convenient measurements from cytoplasmic drops. This system has already been used to characterize a plant channel in terms of diffusion kinetics (Laver & Walker 1987, 1991; Laver, Fairley & Walker, 1989; Laver, 1990) or in terms of the enzymatic model (Fisahn et al., 1986; Bertl, 1989; Draber, Schultze & Hansen, 1991).

The aim of this study is to treat two characteristic properties of this channel by this enzyme kinetic approach in some detail. The first issue is selectivity. It should be pointed out that selectivity of ion channels should not be treated in terms of relative permeabilities as traditionally used for *independent* electrodiffusion of ions across a membrane. The possible transition of different ion species through an individual ion channel is instead expected to take place in a competitive mode and should be treated, therefore, by an appropriate enzyme kinetic formalism. This

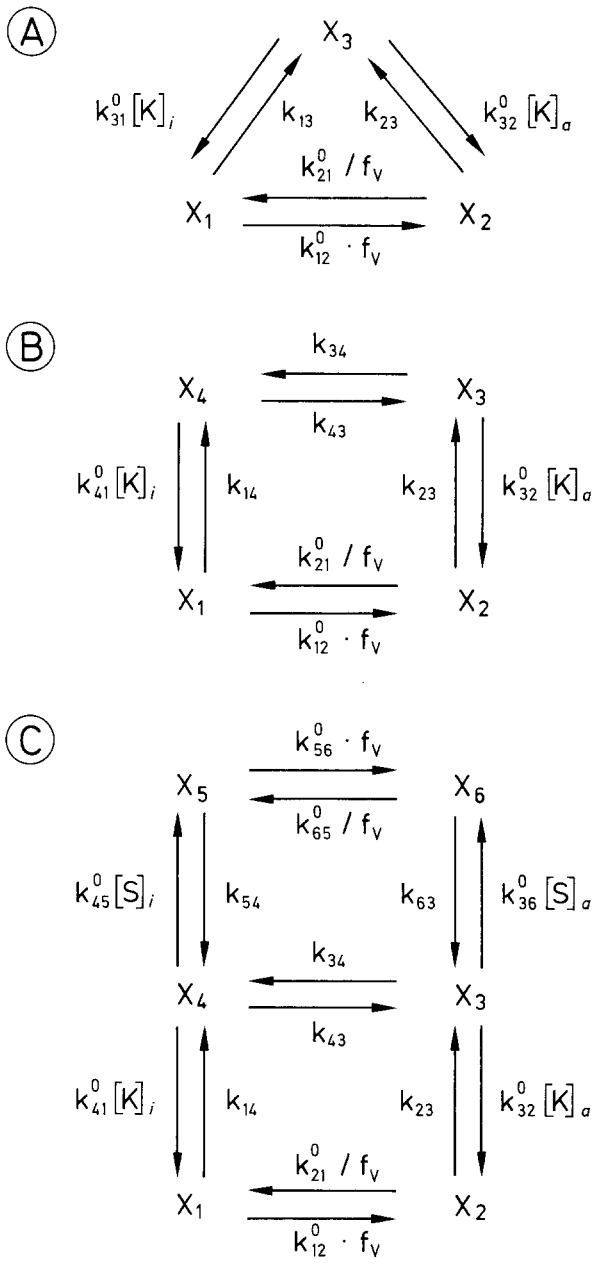


**Fig. 1.** Reaction kinetic models for ion translocation. (*A*) Three reaction steps can account for the substrate concentration $[K^+]_i$ and $[K^+]_o$ at the two sides of the membrane and for the voltage-dependent translocation ($X_1 \leftrightarrow X_2$). (*B*) Model with four states—the two substrate binding steps are uncoupled by reorientation of the unoccupied binding site ($X_3 \leftrightarrow X_4$). (*C*) Extension by an additional transport loop for an alternate substrate, *S*, results in a six-state model which is appropriate to describe competitive transport of two different substrates.

treatment is presented here for the selectivity of the channel for $K^+$ over $Rb^+$.

The second issue is to investigate the effect of competing ions which are not translocated but inhibit the $K^+$ current. This effect of $Na^+$ has already

been interpreted in terms of the enzyme kinetic model (Bertl, 1989), where binding and debinding of $Na^+$ were too fast to be separated. Rather, they entered the calculations by their ratios, the stability constants. The analogous effect of $Ca^{2+}$ has been treated by diffusion kinetics (Laver, 1989), but will be analyzed here in enzyme kinetic terms as well. The main subject of this study, however, is the inhibiting effect of $Cs^+$, which could be resolved with respect to binding and debinding reactions. For this purpose, the blocking and deblocking events of $Cs^+$ were still too short to be analyzed directly, but could be determined by analysis of the statistical fluctuations of the apparent open channel currents. This open channel noise can be analyzed in various ways. Interpretation of power-spectra is a general strategy which has been used by Colquhoun and Ogden (1988), Sine, Claudio and Sigworth (1990), and in several studies by Heinemann and Sigworth (e.g., 1991). For our purpose, a more convenient approach was sufficient, namely fitting of a beta-distribution (Eq. (1)), to the actual amplitude distribution of the current data, according to the theory of FitzHugh (1983) and its application by Yellen (1984). With this method it was possible to determine mean lifetimes of blocked and deblocked states down to 1.5 $\mu$sec.

The resulting blocking kinetics of $Cs^+$ not only followed straightforward (second order) enzyme kinetics, but also provided an example for an intimate linkage between conduction and switching of a channel.

## Materials and Methods

### Materials

*Chara corallina* was grown as previously described (Bertl, 1990). Cytoplasmic drops have been prepared according to Lühring (1986).

The chemicals used (*p.a.* grade) were purchased from Merck (Darmstadt), Serva (Heidelberg), and Sigma (Deisenhofen). Salt solutions have been prepared from 0.1 M or 1.0 M stock solutions with bidistilled water and filtered through 0.22 $\mu$m (Millipore) filters. Amounts of ions were calculated for the desired concentrations. The activities were estimated according to Mohan and Bates (1975), e.g., by activity coefficients of about 0.7 at concentrations of 0.1 M concentrations. Isolated internodia have been stored in artificial pond water (1 mM NaCl, 0.1 mM KCl, 1 mM $CaCl_2$). pH was adjusted with TRIS/MES buffer up to 10 mM. Unbuffered 150 mM KCl solution had pH 5.5. To remove undesired $Ca^{2+}$ (about 0.1 mM contamination in 1 M Merck KCl) EGTA adjusted to pH 7 with TRIS was added to a final concentration of <1 mM. Osmotic differences of solutions with different salt concentrations have been neutralized by addition of sorbitol to the low-salt solution.

### Experimental

Patch-clamp techniques were applied according to Hamill et al. (1981) and Lühring (1986) with a setup as described by Bertl and Gradmann (1987). Electrical asymmetries >10 mV in the measuring circuit have not been tolerated; smaller ones have been neutralized by a compensation device of the measuring amplifier (L/M-EPC 7, List Darmstadt). Liquid junction potentials (amounts within ±5 mV here), as they arise between different solutions in the open pipette and in the bath and disappear when the pipette is closed (Gagne & Plamondon 1983), have been calculated by a general form of the Henderson equation (Quartarao, Barry & Gage, 1987) with mobility data from Robinson and Stokes (1965) for 25°C.

Here, only selected recordings of currents through the prominent tonoplast channel (Lühring 1986; Bertl, 1989) from cell-free patches are given. Unfiltered output signals from the measuring amplifier were stored by a DAT-recorder (DCT-1000 ES Sony) modified (by Fa. Polder, Tettnang) for DC recording and by 20 kHz 8-pole Bessel lowpass filters for in- and output. During the measuring procedure the 3 kHz filtered output signal was monitored by an oscilloscope. The recordings, which have been used for analysis, lasted from a few seconds up to 20 min.

### Analysis

For a visual overview, the data from the recordings have been plotted in a condensed form on a chart recorder. This enabled crude examination of several features, such as baseline-drift, number and activity of channels, and quality of seal. Observations on an oscilloscope allowed a more detailed inspection. Selected portions of the recordings were stored in a microcomputer via an 8-pole Bessel-filter with selectable, fixed corner frequencies (Polder, Tettnang) and a 12-bit D/A-converter (DT 2821, Data Translation). A DC-offset and variable input amplification have been used for adjustment of the output signal to the resolution of the D/A-converter. Open channel currents have been determined from amplitude density histograms.

#### *Current-Voltage Curves*

The data have been analyzed by fitting the parameters of reaction-kinetic models (Fig. 1*B* and *C*) with the equations in Table 1 to the data (*see* Figs. 3, 4, 5, and 7) by a specific cascade of least-square routines using algebraic relationships as given in detail previously (Gradmann et al., 1987). For the model calculations, activities have been used, not concentrations. For computer-mediated data analysis, our own programs have been applied which are not described here in detail.

#### *Open Channel Noise*

The stored data to be analyzed from the DAT-recorder (output filter, $f_D$ = 20 kHz) have been refiltered and resampled into the computer obeying rules and criteria according to Colquhoun and Sigworth (1983). Durations of the main conducting state (ignoring the existence of a minor portion with lower conductances), of bursts (open states with short interruptions according to Colquhoun and Hawkes, 1982) and of closed periods have been determined by computer programs, written according to Sachs,

**Table 1.** Equations for calculations with the six-state model, Fig. 1

A. Auxiliary variables

$$D_{12} = k_{12} \cdot k_{23} + k_{14} \cdot k_{21} + k_{14} \cdot k_{24}$$
$$D_{56} = k_{56} \cdot k_{63} + k_{54} \cdot k_{65} + k_{54} \cdot k_{63}$$
$$k_{4123} = k_{41} \cdot k_{12} \cdot k_{23}/D_{12}$$
$$k_{3214} = k_{32} \cdot k_{21} \cdot k_{14}/D_{12}$$
$$k_{4563} = k_{45} \cdot k_{56} \cdot k_{63}/D_{56}$$
$$k_{3654} = k_{36} \cdot k_{65} \cdot k_{54}/D_{56}$$
$$Q_3 = k_{43} + k_{4123} + k_{4563}$$
$$Q_4 = k_{34} + k_{3214} + k_{3654}$$
$$R_3 = 1 + k_{32} \cdot (k_{12} + k_{21} + k_{14})/D_{12} + k_{36} \cdot (k_{56} + k_{65} + k_{54})/D_{56}$$
$$R_4 = 1 + k_{41} \cdot (k_{12} + k_{21} + k_{23})/D_{12} + k_{45} \cdot (k_{56} + k_{65} + k_{63})/D_{56}$$
$$D_{34} = R_3 \cdot Q_3 + R_4 \cdot Q_4$$

B. Probabilities of the states

$$X_3 = Q_3/D_{34}$$
$$X_4 = Q_4/D_{34}$$
$$X_1 = (X_3 \cdot k_{21} \cdot k_{32} + X_4 \cdot k_{41} \cdot k_{21} + X_4 \cdot k_{41} \cdot k_{23})/D_{12}$$
$$X_2 = (X_4 \cdot k_{41} \cdot k_{12} + X_3 \cdot k_{32} \cdot k_{12} + X_3 \cdot k_{32} \cdot k_{14})/D_{12}$$
$$X_5 = (X_3 \cdot k_{65} \cdot k_{36} + X_4 \cdot k_{45} \cdot k_{65} + X_4 \cdot k_{45} \cdot k_{63})/D_{56}$$
$$X_6 = (X_4 \cdot k_{45} \cdot k_{56} + X_3 \cdot k_{36} \cdot k_{56} + X_3 \cdot k_{36} \cdot k_{54})/D_{56}$$

C. Current equation

$$I = e(X_1 k_{12} - X_2 k_{21}) + e(X_5 k_{56} - X_6 k_{65}) = e \cdot \frac{Q_3 k_{34} - Q_4 k_{43}}{Q_3 R_3 - Q_4 R_4}$$

D. Equations for blocking

| | | |
|---|---|---|
| Probability of unblocked state | $P_o = X_1 + X_2 + X_3 + X_4$ | |
| Probability of blocked state | $P_c = X_5 + X_6 = 1 - P_o$ | |
| Blocking rate; mean open time | $k_b = (X_4 \cdot k_{45} + X_3 \cdot k_{36})/(X_1 + X_2 + X_3 + X_4)$; | $\tau_o = 1/k_b$ |
| Deblocking rate; mean closed time | $k_d = (X_5 \cdot k_{54} + X_6 \cdot k_{63})/(X_3 + X_4)$; | $\tau_c = 1/k_d$ |
| Open probability | $P_o = \tau_o/(\tau_o + \tau_c)$ | |

Neil and Barkakati, (1982), Sachs (1983) and Vivaudou, Siger and Walsh (1986).

If the mean open and/or closed times are shorter than the filter time constant, the full amplitudes of the individual events are not resolved any more. In this case, the mean open and closed times ($\tau_o$ and $\tau_c$) can partially be reconstructed by fitting of a beta-distribution (Eq. 1), to the actual amplitude distribution of the current data, according to the theory of FitzHugh (1983) and its application by Yellen (1984). Briefly:

The density function $Y(x)$ of the relative amplitudes $x$ ($0 < x < 1$) of a rectangular signal after low-pass filtering with a filter time constant $\tau$, reads

$$Y(x) = \frac{x^{a-1}(1-x)^{b-1}}{B(a,b)} \tag{1}$$

with

$$B(a,b) = \int_0^1 x^{a-1}(1-x)^{b-1}dx \tag{2}$$

$$a = \tau/\tau_o, \text{ and } b = \tau/\tau_c, \tag{3}$$

The parameters $a$ and $b$ determine the shape of the distribution, and the beta-function $B(a,b)$ scales the integral of the beta-distribution to unity. The relative frequency $H(x)$ of the amplitudes in the interval $(x, x + \delta x)$ is approximately $H(x) = Y(x) \cdot \delta x$ for small $\delta x$. In order to apply the theory (for 1-pole filters) to our measurements with an 8-pole Bessel filter with the frequency $f_B$, empirical calibration was carried out with known rectangular signals, yielding $\tau = 0.224/f_B$ for our apparatus.

For practical application, the theoretical distribution has to be convoluted by the noise of the apparatus which can be determined by fitting a Gaussian normal distribution, $G(i)$, with the standard deviation $s$

$$G(i) = \frac{1}{s\sqrt{2\pi}} \exp\left(-0.5\frac{i^2}{s^2}\right) \tag{4}$$

to the distribution of the scattered current data of the baseline (between bursts). The real histogram $H$ is now the convolution sum

$$H(i) = \sum_{j=-N}^{+N} G(j)H_0(i+j) \tag{5}$$

of the pure (zero noise) beta-distribution $H_0$ and the noise distribu-

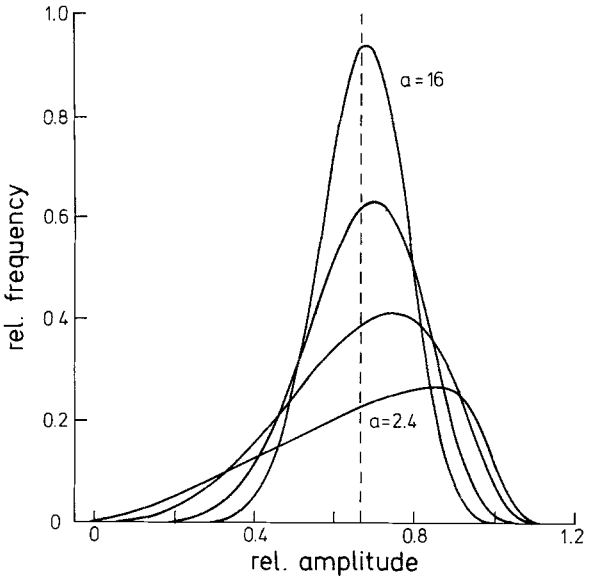


**Fig. 2.** Theoretical amplitude distribution of a filtered (time constant $\tau$) signal switching between 1 (here open state with a mean lifetime $\tau_o$) and 0 (here closed state with a mean lifetime $\tau_c$), convoluted with a Gaussian noise with standard deviation of 10% of the full amplitude; at a constant ratio $a/b = \tau_o/\tau_c = 2$, between the two parameters of the beta-distribution, different values of $a = \tau/\tau_c$ (2.4, 4, 8, and 16) demonstrate the effect of increasing filtering; broken line: mean.

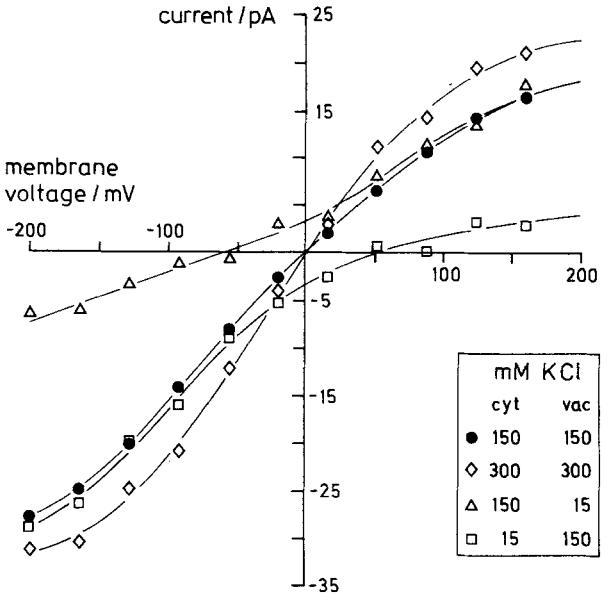


**Fig. 3.** Current-voltage-curves of the open channel under various conditions for $K^+$ uniport; measurements from excised patches at pH 7 with 1 mM EGTA; data points are means from different measurements; curves are least-square fitted by the four-state model in Fig. 1*B* with the corresponding eight parameters listed in Table 2 (first column, upper part).

tion $G(j)$. The number of the coefficients $N$ was chosen to cover a range of six standard deviations. Figure 2 shows some examples of how, for decreasing filtering (or increasing speed of flickering), this noisy beta-distribution peaks closer and closer to the mean, $\tau_o/(\tau_o + \tau_c)$, and becomes more and more symmetric and narrow in shape, eventually approaching the shape of the baseline noise. The two parameters $a$ and $b$ could well be determined if they were confined within the range between 2 and 15 by appropriate filtering.

The reaction kinetic model for the description of the experimental data is given by Fig. 2 and by the equations in Table 1.

## Conventions and Definitions

In this study simply "current-voltage curve" is used for the steady state, current-voltage relationship of the predominant $K^+$ channel in its prime open state. According to physiological tradition, we apply the following sign convention also to the vacuolar membrane: the voltage, $V_m$, across a membrane which separates a cytoplasmic compartment from a noncytoplasmic one, is the electrical potential in a cytoplasmic compartment minus the electrical potential in the extracytoplasmic compartment; correspondingly, the movement of positive charges from the cytoplasmic compartment to the extracytoplasmic compartment is a positive (outward) current.

The mean probability for a transition from state $X_i$ to state $X_j$ within a given time span is the rate constant $k_{ij}$. For substrate binding, the effective rate constant is the product $k_{ij}^0 \cdot [S]$ between the fundamental rate constant $k_{ij}^0$ and the chemical activity [S] of the substrate. For a reaction which describes the movement of the charge $z \cdot e$ from $X_i$ to $X_j$ along the the fraction $d$ of the membrane voltage $V_m$, the effective rate constant $k_{ij}$ is the product between the reference rate constant $k_{ij}^0$ at zero voltage and an electrical weighting factor $f_V$ which accounts for the exponential voltage characteristics of an Eyring barrier

$$k_{ij} = k_{ij}^0 \cdot f_V = k_{ij}^0 \cdot \exp(z \cdot d \cdot x \cdot V_m/V_0)$$
$$= k_{ij}^0 \exp(z \cdot e \cdot d \cdot x \cdot V_m/(k \cdot T))) = k_{ij}^0 \exp(V_{ij}/V_0), \quad (6)$$

where $x$ ($0 < x < 1$) describes the shape of the energy barrier for $k_{ij}$, and $(x - 1)$ for the back-reaction $k_{ij}$ (here, $x$ is always 0.5 as an initial, simplifying assumption, which corresponds to symmetry), and $V_0 = k \cdot T/e$ (= 25.5 mV at 23°C), with $z$, $e$, $k$, and $T$ having their usual thermodynamic meanings. Thus for voltage-dependent binding, the effective rate constant would be the product of $k_{ij}^0$ and the electrochemical activity $[S] \cdot f_V$.

## Results

### $K^+/Rb^+$ Selectivity

The prime $K^+$ channel from the tonoplast of *Chara* has one predominant conducting state on which we focus here. In rare cases (about 0.1%), the channel did also appear in various alternate states with lower conductance levels.

Figure 3 shows the current-voltage relationships of the open channel under various $K^+$ conditions. In symmetrical 150 mM KCl, which is used as the

reference condition, the current-voltage curve is sigmoid with a larger amount for the negative saturation current than for the positive one. This asymmetry can be used to identify the channel and its orientation in the patch.

Saturation of the current at large voltage displacements from equilibrium can have various reasons. One familiar mechanism is substrate depletion by limited diffusion from the bulk solution to the binding site. In this case, the size of the saturation currents should be proportional to the substrate concentration in the charge delivering compartment. Consequently, in symmetrical 300 mM KCl the saturation currents should be twice as large as under reference conditions. However, the results disprove this possibility because the observed increase is only about 1.2-fold.

Another possibility for the observed curvature is voltage-dependent blockade by a competing substrate. In fact, the channel under investigation here, exhibits this effect in the presence of various cation species, such as $Ca^{2+}$ (Laver 1990; Laver & Walker 1991, and this study), $Cs^+$ (*for details see below*) or $Na^+$ (Bertl, 1989). However, in the absence of alternate cations (except negligible amounts of $H^+$), in particular under complexation of $Ca^{2+}$ by EGTA, saturation is still evident. On the other hand, kinetic limitation by the enzyme itself, as examined by fitting the model to the data (compare points and curves), provides a satisfying description.

For further investigation, the current-voltage curves have also been measured under asymmetric (15/150 mM) KCl conditions for either direction. The results in Fig. 3 show that the reversal voltages behave like those of ideal $K^+$ electrodes, indicating a high selectivity of the channel for $K^+$ over $Cl^-$.

Furthermore, a decrease of the substrate concentration at one side of the membrane does not cause a significant increase of the saturation current towards this side. This phenomenon, which is found for either direction here, is equivalent to a lack of "transinhibition" (it is called transinhibition, if an increase of the substrate concentration on one side causes a decrease of the saturation flux towards this side—or *vice versa* for a decrease in substrate concentration as applied here). Transinhibition indicates coupling between the two binding/debinding reaction steps at the two sides of the membrane, and could readily be described by the reaction scheme (Fig. 1*A*). The apparent lack of transinhibition found here, is incompatible with this simple reaction scheme. However, when these two equilibrium reactions are assumed to be separated by an extra reaction step for the reorientation of the empty binding site, the coupling will be weak, and little or no transinhibition will be observed. The latter model with an extra reaction step (Fig. 1*B*) does provide a good description of the experimental results.

The results in Fig. 3 are relevant with respect to another issue which has not been investigated systematically here: The successful model (Fig. 1*B*) employs only one voltage-dependent reaction step, whereas in more popular models the membrane voltage is shared by at least two voltage-dependent translocation steps (in case of single-file diffusion with a minimum of 2 binding sites in series) plus the two binding/debinding reactions which are usually considered to take place within the electrical gradient as well. In such a long series of reactions, the individual reactions are subjected to only fractions of the entire voltage, which makes each one relatively insensitive to the entire membrane voltage. Consequently, the series of rather linear voltage dependencies will result in a rather linear current-voltage curve (*see* Hille, 1984). However, the pronounced curvatures of the experimental results in Fig. 3 do not support such a serial splitting of the membrane voltage. Rather, the fits suggest that the conceptually more simple model with only one voltage-dependent step (Class-I model) is not only sufficient but also more appropriate than a model with significant voltage-dependence in the substrate binding/debinding reaction steps. The latter situation could be expected, however, at low substrate concentrations.

The numerical results of fitting the set of eight parameters of the four-state model in Fig. 1*B* to the data in Fig. 3, are listed in Table 2 together with data for $Rb^+$ transport, and comparable data from other studies. On algebraic grounds (Gradmann et al., 1987), there is a unique set of parameters which satisfies the data from the reference curve and of the current-voltage curves from the two asymmetric conditions, whereas data from symmetric 300 mM KCl may serve as controls or predictions. Actually, the model has been fitted to the entire ensemble of data, and the statistical significance of the individual numbers in Table 2 has not been explored.

The transport kinetics of $Rb^+$ have been investigated because $Rb^+$ is expected to be an alternate substrate which competes with $K^+$ for the binding site of the channel. The results are shown in Fig. 4 together with the reference curve (symmetric 150 mM KCl). The results from biionic conditions, i.e., when $K^+$ was completely replaced on one side by $Rb^+$, show that $Rb^+$ is translocated by the channel as well, though to a lesser extent. The finding that the saturating $Rb^+$ currents are the same under biionic conditions and under symmetrical conditions, points again to a suppressed coupling of the $Rb^+$ binding equilibria on the two sides of the membrane—same as for $K^+$ mentioned above.

**Table 2.** Reaction kinetic parameters of the prime $K^+$ channel from the tonoplast of *Chara*, and of the plasmalemma of guard cell protoplasts of *Vicia faba*

| Mean transition probability | *Chara* tonoplast | | *Vicia* plasmalemma[c] |
|---|---|---|---|
| | No $Ca^{2+}$[a] | 0.1 mM $Ca^{2+}$[b] | |
| $K^+$ translocation $i \rightarrow o$ | 1,410 | 12,700 | 149 |
| $K^+$ translocation $o \rightarrow i$ | 3,370 | 2,625 | 204 |
| $K^+$ binding outside | 10,500 | 6,600 | 1,746 |
| $K^+$ debinding outside | 106,000 | 52,644 | 9,456 |
| $K^+$ binding inside | 5,300 | 4,913 | 2,618 |
| $K^+$ debinding inside | 15,800 | 78,750 | 8,279 |
| Reorientation of binding site $i \rightarrow o$ | 270 | 250 | 32 |
| Reorientation of binding site $o \rightarrow i$ | 194 | 113 | 28 |
| $S^+$ translocation $i \rightarrow o$ | 498 | | 6 |
| $S^+$ translocation $o \rightarrow i$ | 4,510 | | 10 |
| $S^+$ binding outside | 403 | | 241 |
| $S^+$ debinding outside | 4,070 | | 694 |
| $S^+$ binding inside | 300 | | 104 |
| $S^+$ debinding inside | 240 | | 322 |

[a] This study. [b] (Bertl, 1989). [c] (Gradmann et al., 1987).
Parameters of the four-state model for uniport and for an alternate substrate $S^+$, i.e., $Rb^+$ in this study and $Na^+$ for the *Vicia* channel; data in $10^6$ $sec^{-1}$ at reference conditions (1 M substrate and zero voltage).

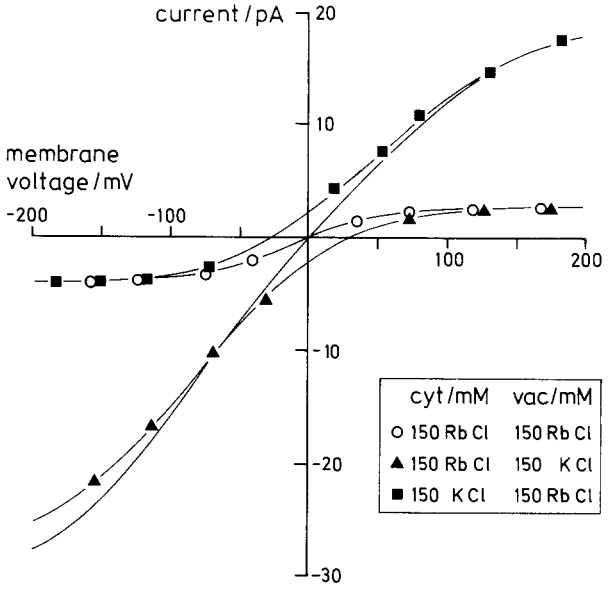


**Fig. 4.** Current-voltage-curves of the open channel under biionic and symmetrical $K^+$ and $Rb^+$ conditions as marked; measurements from excised patches at pH 7 with 1 mM EGTA; data points are means from different measurements; curves are least-square fitted with the six-state model in Figs. 1*C* (current equation Table 1*C*) with the fourteen parameters as listed in first column of Table 2 (eight parameters from experiments to Fig. 3 plus six parameters for the $Rb^+$ loop from these data), reference curve with symmetrical 150 mM KCl without symbols.

The analysis of these data by fitting the kinetic parameters of the second transport loop of the model in Fig. 1*C* to the measured data, provided the numerical results listed in Table 2. The fitted model curves agree well with the experimental data. The reversal voltages under biionic conditions of opposite sign turned out to be not equivalent: about 30 mV when internal $K^+$ was replaced by $Rb^+$, and about $-20$ mV for the symmetrical arrangement.

## Blocking

The current-voltage curves for biionic conditions ($K^+/Cs^+$) in Fig. 5 show that $Cs^+$ is not translocated in either direction by the channel, that $Cs^+$ on one side (*cis*) does not affect the $K^+$ (saturation) currents from the opposite (*trans*) side, and that the outward-current at $K^+$ inside and $Cs^+$ outside, steeply falls to zero at negative voltage. The data in Fig. 5 are well fitted by the curves calculated by the model in Fig. 1*C* and Table 1 with the parameters listed in Tables 2 and 3.

Figure 6 shows the reference current-voltage curve (symmetric 150 mM KCl, without symbols) and its changes upon addition of various amounts of $Cs^+$ symmetrically to both sides of the membrane. The fact that the outward ($K^+$) currents are hardly affected does not only confirm the lack of a transef-

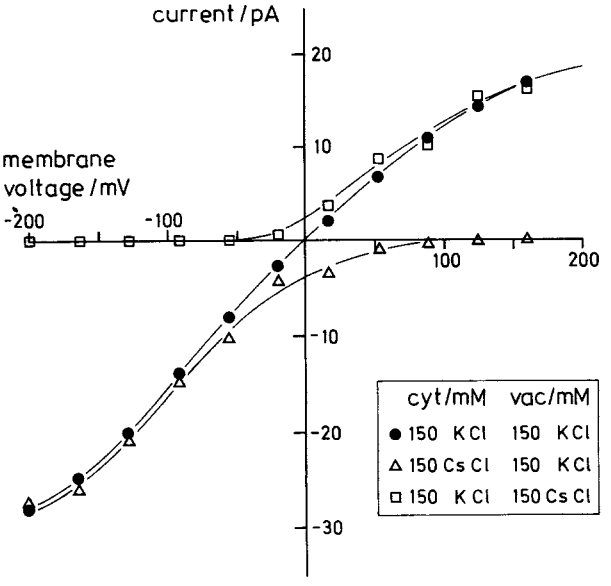


**Fig. 5.** Open-channel current-voltage relationships of the prime $K^+$ channel from the tonoplast of *Chara* in isolated patches under symmetric (150 mM) $K^+$ conditions (reference) and under biionic $K^+/Cs^+$ conditions; all solutions with 1 mM Tris/EGTA at pH 7; points measured, curves fitted by model in Fig. 1*C* with parameters listed in Tables 2 and 3; main result: $Cs^+$ not translocated by the channel; additional observation: sharp bending to zero current in negative voltage range.

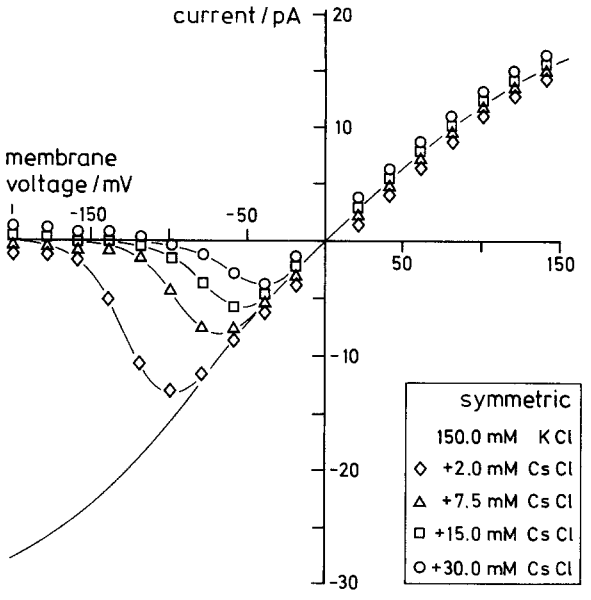


**Fig. 6.** Open channel current-voltage relationships of the prime $K^+$ channel from the tonoplast of *Chara* in isolated patches under symmetric (150 mM) $K^+$ conditions without (reference curve without symbols) and with various amounts of $Cs^+$ added at both sides of the membrane; all solutions with 1 mM Tris/EGTA at pH 7; points measured, curves fitted by model in Fig. 1*C* with parameters listed in Tables 2 and 3; main results: $Cs^+$ affects only inward ($K^+$-) current, namely by steeply progressive inhibition for increasing (negative) voltages; for graphical reasons, coinciding symbols for the same currents are separated vertically.

fect of external $Cs^+$ on the $K^+$ outward current (*compare* Fig. 5), it means, in addition, that internal $Cs^+$ does not compete with $K^+$ for the inward-oriented binding site.

The most striking feature of Fig. 6, however, is the inhibition of the $K^+$ inward currents by external $Cs^+$. This inhibition proceeds with the amount of (negative) voltage. At small (negative) voltages, the ratio between the currents with and without $Cs^+$ is almost 1, but for larger voltage displacements, it decays to zero. This voltage-dependent inhibition cooperates with the amount of $Cs^+$: for increasing $Cs^+$ concentrations (2, 7.5, 15 and 30 mM) the voltage for 50% inhibition is reached at progressively smaller amounts of voltage displacement (about $-130$, $-90$, $-70$, and $-50$ mV, respectively) from equilibrium. As a consequence, the current-voltage curves have a current-minimum (maximum amount of inward current) which falls in amplitude and distance from equilibrium, with increasing $Cs^+$ outside. The kinetics of this feature is treated in more detail below, on the basis of the model in Fig. 1. The stability constants $K^0$, the charge number, $z$, and the effective voltage fraction, $d$, which can be determined from model fits to the steady-state data, are listed in Table 3, together with corresponding data from other ions.

A similar effect of $Na^+$ on the $K^+$ currents through this channel, which has already been analyzed with the model in Fig. 1*C* (Bertl, 1989), will be discussed. Also, $Ca^{2+}$ is known to inhibit the $K^+$ currents through this channel with comparable voltage characteristics (Laver, 1989). It is examined here, whether these characteristics can also be described by the model in Fig. 1*C*. For this purpose, the effect of $Ca^{2+}$ on the $K^+$ currents has been measured once more, this time under conditions which allow a direct comparison of the results (Fig. 7) with other data presented here. The data in Fig. 7 are, in fact, well described by the model in Fig. 1*C* with the parameters listed in Tables 2 and 3. According to this analysis (and already by direct inspection of the data) it can be seen that $Ca^{2+}$ inhibits the $K^+$ currents from both sides of the membrane progressively with the voltage-displacement (either sign) from the equilibrium; but these effects are asymmetrical. At zero voltage, $Ca^{2+}$ forms inside a more stable complex at the binding site of the channel than outside. On the other hand, these two $Ca^{2+}$ effects are similar with respect to their weak voltage sensitivity (*d:* 0.17 and 0.2) compared to the high voltage sensitivity of the $Cs^+$ blockade from outside (*d:* 2).

**Table 3.** Effects of various substrates on reaction system of $K^+$ uniport, in terms of model in Fig. 1*B* and *C* (equations in Table 1)

| | | Inside | | | Outside | | |
|---|---|---|---|---|---|---|---|
| A. Stability constants, charge number, and voltage dependence | | | | | | | |
| Substrate | Transported | $K^0$ | $z$ | $d$ | $K^0$ | $z$ | $d$ |
| $Na^+$ | no | 8.9 $M^{-1}$ | 1 | 1.0 | 1.1 $M^{-1}$ | 1 | 0.4 |
| $K^+$ | yes | 0.33 $M^{-1}$ | 1 | 0 | 0.10 $M^{-1}$ | 1 | 0 |
| $Rb^+$ | yes | 1.25 $M^{-1}$ | 1 | 0 | 0.1 $M^{-1}$ | 1 | 0 |
| $Cs^+$ | no | 0 | | | 46 $M^{-2}$ | 2 | 1 |
| $Ca^{2+}$ | no | 250 $M^{-1}$ | 2 | 0.2 | 10 $M^{-1}$ | 2 | 0.17 |
| B. Rate constants | | | | | | | |
| $Cs^+$ binding outside | | | | | $92 \cdot 10^6$ $sec^{-1} \cdot M^{-2}$ | | |
| $Cs^+$ debinding outside | | | | | $2 \cdot 106$ $sec^{-1}$ | | |

A: Stability constants, $K_i^0$, and their voltage dependencies ($z$ and $d$, *see* Eq. 6) of several transported and nontransported substrates for binding inside and outside; $Na^+$ data (from Bertl, 1989); B: Rate constants for $Cs^+$ blocking and deblocking, both with $d = 1.0$ and $z = 2$ (*see* Eq. 6), for $V = 0$.

The phenomenon of voltage-enhanced blocking by an alternate ion which competes with $K^+$ for the binding site, has been analyzed for the case of $Na^+$ (Bertl, 1989) and $Ca^{2+}$ (above) in terms of voltage-dependent stability constants of the nontranslocated competitor for the two binding reactions at the two sides of the membrane (Table 3). In the presence of $Cs^+$, the $K^+$ currents do not only appear to be reduced in their steady-state amplitude, they show also remarkably increased noise (*not shown*). The flickering appearance of the current in the presence of $Cs^+$, may be explained by short (and complete) blockages of the normal open channel current which are incompletely resolved by the apparatus. Under this aspect, the apparently noisy open channel current would, in fact, be a burst.

The information from the (in general) asymmetrically enlarged noise has been used to fit the parameters of this hypothetical switching mechanism (mean open time and mean closed time) to the data. Figure 8 shows an example of an amplitude histogram from such a scattered current, measured in the presence of $Cs^+$, as well as the much narrower current distribution of the baseline. The similarity between the wide distribution of the burst currents and the theoretical curves of beta-distributions in Fig. 2 is evident. Fitting $a$ and $b$ via Eq. (1) to the current histograms of the bursts at various voltages and in the presence of various amounts of $Cs^+$, resulted in the mean lifetimes of the on- and off-periods within these apparent bursts. The result are listed in Table 4 with statistical information and plotted in Fig. 9 with the model curves as they result by fitting the rate constants for binding and debinding of $Cs^+$ (Table 3) to and from

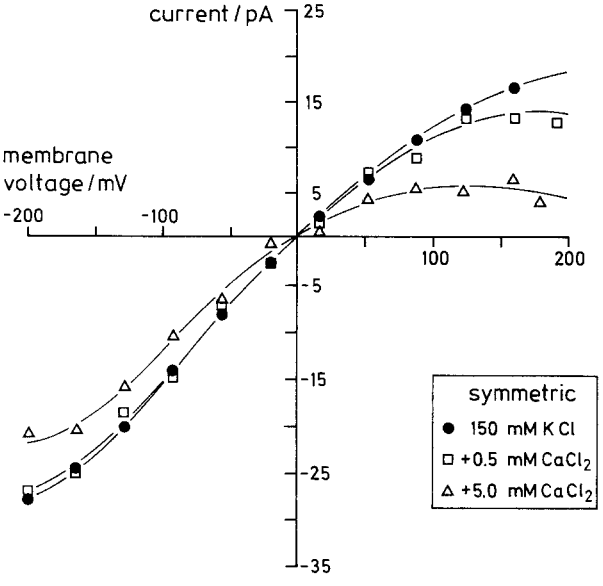


**Fig. 7.** Open channel current-voltage relationships of the prime $K^+$ channel from the tonoplast of *Chara* in isolated patches under symmetric (150 mM) $K^+$ conditions without (reference-curve) and with two different amounts of $Ca^{2+}$ added at both sides of the membrane; all solutions with 3 mM Tris/Mes at pH 7; points measured, curves fitted by model in Fig. 1*C* with parameters listed in Tables 2 and 3; main results: $Ca^{2+}$ affects predominantly outward ($K^+$-) current, namely by gently progressive inhibition for increasing (positive) voltages.

the outside-oriented binding site of the reaction cycle for potassium uniport (Table 2).

Analysis of the mean open time ($\tau_o$) of the channel (in the absence of blocker) which may correspond to the mean burst duration ($\tau_B$, in the presence of

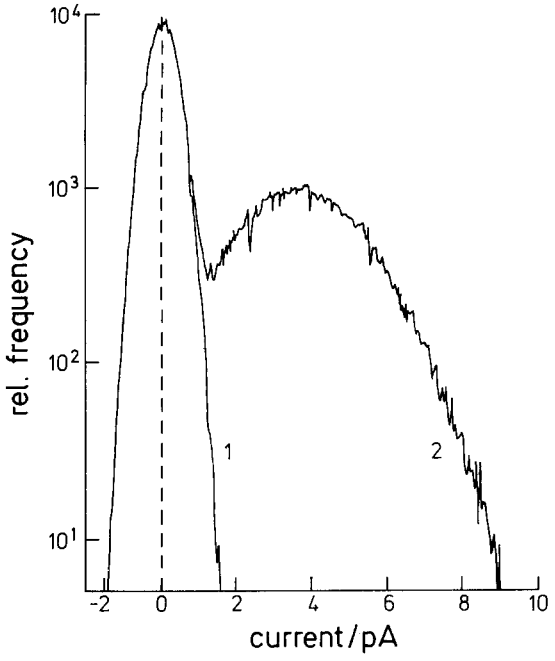


**Fig. 8.** Semilogarithmic amplitude histogram of a (flickering) open channel current recording from the prime $K^+$ channel in the tonoplast of *Chara* in isolated patch in symmetrical 150 mM KCl and 7.5 mM CsCl at −40 mV; entire histogram comprises recordings of baseline (1) and of one (flickering) open channel; filter time constant 150 μsec; without $Cs^+$, the mean open channel current under these conditions is about -8 pA (*compare* Fig. 5).

**Table 4.** Mean open times ($\tau_o$) and mean closed times ($\tau_c$) at different membrane voltages ($V_m$) and different $Cs^+$ concentrations symmetrically at both sides of the membrane with 150 mM KCl

| $V_m$/mV | 7.5 mM $Cs^+$ | 15 mM $Cs^+$ | 30 mM $Cs^+$ |
|---|---|---|---|
| | $\tau_o$/μsec<br>$\tau_c$/μsec | $\tau_o$/μsec<br>$\tau_c$/μsec | $\tau_o$/μsec<br>$\tau_c$/μsec |
| −110 | 7.6 ± 2.1<br>39.0 ± 9.3 | | |
| −100 | 10.6 ± 2.8<br>26.2 ± 6.7 | 2.6 ± 0.9<br>25.7 ± 6.7 | |
| −90 | 14.7 ± 3.6<br>17.6 ± 3.1 | 3.7 ± 1.9<br>16.7 ± 3.9 | |
| −80 | 20.5 ± 5.2<br>10.7 ± 3.0 | 5.13 ± 1.3<br>11.9 ± 2.8 | |
| −70 | 28.7 ± 7.3<br>8.0 ± 1.7 | 7.2 ± 1.8<br>7.9 ± 2.1 | 1.8 ± 1.8<br>8.7 ± 2.0 |
| −60 | | 10.1 ± 2.6<br>5.4 ± 1.3 | 2.5 ± 0.6<br>5.0 ± 1.3 |
| −50 | | 14.3 ± 3.6<br>3.1 ± 1.4 | 3.6 ± 0.9<br>3.6 ± 1.3 |
| −40 | | 20.3 ± 5.2<br>2.6 ± 2.1 | 5.1 ± 2.1<br>2.3 ± 1.1 |
| −30 | | | 7.2 ± 1.8<br>1.6 ± 1.9 |

Results of fits of beta-distributions to amplitude histograms of bursts; filter time constants for experiments with 7.5, 15, and 30 mM $Cs^+$: 150, 70, and 30 μsec, respectively; means and standard deviations from three to five determinations.

blocker) revealed one predominant component and a minor one, e.g. at −150 mV the distribution of lifetimes consisted of 91% of a 23-msec component ($\tau_o$) and 9% of a 2.5-msec component ($\tau_{o'}$). Both components have a maximum duration at about −150 mV (data for $\tau_o$ in Table 5). The minor component will be ignored in the following.

The mean burst durations ($\tau_B$, in the presence of 30 mM $Cs^+$) have also been determined at different membrane voltages. A comparison of $\tau_o$ and $\tau_B$ with their voltage dependence (Table 5) shows that these two parameters essentially coincide at each voltage, i.e., $Cs^+$ blockade does not prolong the bursts compared to the mean duration of the unblocked open state.

## Discussion

### General Aspects

The results may be summarized by the global statement that the used model is appropriate to describe the kinetics of the channel not only as a uniporter, but also for competition of different substrates. *Appropriate,* means an unambiguous relationship between the experimental results and the model. It is a benefit of the model, that—under favorable circumstances—it may shrink and grow according to the availability of experimental information and still be appropriate. To achieve this benefit, three assumptions have been made: (i) There is only one substrate binding site of the channel. (ii) Translocation of the substrate is the only voltage-dependent reaction of the enzymatic cycle. (iii) The binding site is reoriented by a conformation change which

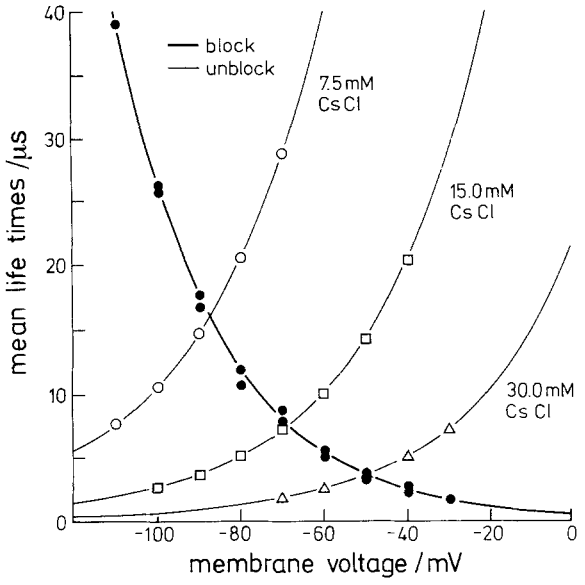


**Fig. 9.** Mean open and closed times during the (flickering) open channel current as function of the voltage at different $Cs^+$ concentration; 150 mM KCl and additional CsCl symmetrical in all experiments; points are measured, curves are fitted by model in Fig. 1*C* (equations in Table 1) with parameters listed in Table 1 (for $K^+$ uniport) and Table 3*C* (for $Cs^+$ blockage).

may become rate limiting. The additional assumption, $x = 0.5$, which stands for symmetry of the Eyring barrier, is commonly used for the sake of convenience, as long as the treatment with an asymmetric barrier is not required explicitly.

The present study does not claim that these properties *do* hold for the channel under investigation or even other channels. It only claims that for an appropriate kinetic description of this channel, some details may be ignored which are known from different sources to hold for other channels. Nevertheless, the results suggest that these properties *may* hold in the first place. Draber et al. (1991) have even shown that an enzyme kinetic treatment of the type used here is superior in describing the anomalous mole fraction effect (of the very $K^+$ channel from *Chara*) compared to the traditional single-file diffusion model of Hille and Schwarz (1978). Thus, the used enzyme kinetic approach does not only seem to be acceptable, it may even point to some unexpected but genuine properties of the channel.

Commenting on the numerical results, the rate-limiting step in either direction is the reorientation of the empty binding site which may correspond to a conformation change, the fastest processes of the system are the debinding reactions (up to $10^{11}$ $sec^{-1}$), and substrate binding in the order of $10^{10}$ $sec^{-1}$ $M^{-1}$ turns out to be very fast as well.

It is not unexpected that the equilibrium reactions are fast compared to the rate-limiting reorientation steps, which do actually reflect the enzymatic processing reactions. The small transinhibition effects render the discrepancy between the velocities of equilibration and reorientation that dramatic (Gradmann et al., 1987). Actually, the resulting velocities around $10^{10}$ $sec^{-1}$ $M^{-1}$ for $K^+$ binding seem to be at or even beyond the limits of physical possibility. In this context, an alternate explanation for absent transinhibition should be mentioned, namely that the empty binding site was (negatively) charged and the loaded binding site was electroneutral (Gradmann et al., 1987). In this case, an equivalent set of unique rate constants cannot be determined from current-voltage curves (Gradmann et al., 1987). For this reason, the formalism with neutral binding site and charged complex (Fig. 1) has been preferred here.

**Table 5.** Mean open times ($\tau_o$) in the absence of $Cs^+$, and mean burst time ($\tau_B$) in the presence of 30 mM $Cs^+$, at various membrane voltages $V_m$

| $V_m$/mV | $\tau_o$/msec | $\tau_B$/msec |
|---|---|---|
| −200 | 6.3 ± 1.6 | 6.0 ± 1.5 |
| −150 | 19.3 ± 5.2 | 20.7 ± 4.9 |
| −100 | 14.5 ± 3.7 | 13.1 ± 3.4 |
| −80 | 5.4 ± 1.4 | 5.0 ± 1.3 |

$Cs^+$ symmetrical at both sides of the membrane with 150 mM KCl, pH 7; means and standard deviations from three to five determinations.

For comparative purposes, the first part of Table 2 shows the reaction kinetic parameters for uniport determined here with those from related studies. In general, the results of Bertl (1989) are confirmed; only the $K^+$-channel complex inside seemed to be destabilized by $Ca^{2+}$ according to the two increased rate constants for $K^+$ translocation from inside to outside and for $K^+$ debinding inside. The inhibitory effect of $Ca^{2+}$ on the $K^+$ currents far from equilibrium (especially in the positive voltage range), as expressed by smaller rate constants for the reorientation of the empty binding site (especially from outside to inside), is already known (Laver, 1990), and can also be interpreted in terms of the model used here.

It should be noted that the $Ca^{2+}$ concentrations on the cytoplasmic side used for the experiments in Fig. 7, are far above the physiological range. Thus, the described effects may be irrelevant for the intact cell, but relevant for biophysicists and also for physiologists who frequently use such high $Ca^{2+}$ concentrations to facilitate seal formation in the curse of patch-clamp experiments.

The rate constants from the plasmalemma chan-

nel in *Vicia faba* are in general smaller but consistent with those from the *Chara* tonoplast with respect to fast binding/debinding reactions inside and outside, rate-limiting reorientation of the empty binding site, and intermediately fast translocation (at zero voltage).

## Selectivity

The results about possible transport of alternate cations ($Rb^+$ in the *Chara* tonoplast and of $Na^+$ in the *Vicia* plasmalemma) through a $K^+$ channel are listed in the lower part of Table 2. It would be premature to discuss here the similarities and dissimilarities which can be found between these sets of data, because it is not clear whether the differences are due to the nature of the alternate substrates ($Rb^+$ has a larger and $Na^+$ a smaller atomic radius compared to $K^+$), or due to differences between the channels of different origin (or a combination thereof).

However, the general success of this approach also for substrate competition, offers some explanations, e.g., for the problem of apparently inconsistent reports on *relative permeabilities*, in particular of $Rb^+$ compared to $K^+$. Bona fide application of the familiar Goldman-Huxley-Katz equation to the data in Fig. 4 would, in fact, also result in numerical inconsistencies: as judged by the different amounts of reversal voltages, the relative permeability of $Rb^+$ would be either about 0.3 or about 0.5, and judged by the transport rates far from equilibrium, smaller and again different coefficients would result for the discrimination of $Rb^+$ over $K^+$. In contrast, the model in Fig. 1*C* provides a consistent and complete description for a wide range of experimental conditions.

## Some Physical Interpretations

Some results of our analysis may be interpreted in physical terms. Table 3 shows that binding and debinding of transported substrates ($K^+$ and $Rb^+$) can be assumed to be voltage independent ($d = 0$), whereas the nontransported ligands require a voltage dependence of the binding/debinding ($d$ between 0.17 and 1) for the increase of the inhibition with voltage. One might imagine that $K^+$ and $Rb^+$ reach the transport site easily, whereas the blocking ions plug the pore and cause the part $d$ of the voltage drop across the membrane to occur not at the enzymatic transport cycle any more but at a new locus of high resistance, namely the plug. We do not favor this mechanistic model, in general, because such macroscopic terms seem to be inappropriate for the behavior of single ions in their microscopic environment, and, in detail, because with that mechanistic model, some kinetic details are difficult to explain, such as the stoichiometry of the $Cs^+$ blockade, or the identity of the binding site for translocated and blocking ligands in the model.

Nevertheless, the results allow a physical interpretation of the asymmetric effect of the different blockers. The relatively large effects of $Na^+$ and of $Ca^{2+}$ inside, indicate a high density of local charges inside which provide a strong electric field to remove the tight hydrate shells from $Ca^{2+}$ with its double charge or from $Na^+$ with its small atomic radius. Correspondingly, the interaction of the large $Cs^+$ is weak inside but strong outside, where a weak electric field suffices to dehydrate the ions with a large ionic radius. These relationships correspond to the validity of the Eisenman-series Nr. XI inside and Nr. I outside (Eisenman, 1962).

## Switching Kinetics

For the description of the voltage dependence of the switching kinetics of the $Cs^+$ blockade (Fig. 9), the charge number for binding and debinding of $Cs^+$ was $z = 2.0$, and the effective voltage fraction $d = 1$. When the data in Table 4 were fitted by a more common relationship of the H. Woodhull (1973) form $\tau_j = \tau_j^0/(1 + f_V \cdot K_j)$, with $f_V = \exp(z_j \cdot d_j \cdot x \cdot V_m/(25.5\ \text{mV}))$ at 23°C, an optimum $z_j \cdot d_j = 1.8$ was found. For most purposes, this discrepancy between 1.8 and 2.0 would probably not matter. In our context, it seems just to favor our approach. This discrepancy becomes qualitatively plausible by the fact that in the common approach only one voltage-dependent reaction step for gating is regarded (bindingand debinding of $Cs^+$), independent of the transport characteristics of the open channel, whereas in our approach these processes are not treated independently but comprise the voltage dependence of the $K^+$ translocation step (with $z \cdot d = 1$) as well (for equations *see* Table 1).

A corresponding conclusion can be reached from a comparison of the mean open times in the absence of blocker with the mean burst durations in the presence of a blocker (Table 5). If the blocker would act on the normal "open/closed" gating switch, the transition between open and closed would take place more seldom when the probability of the open state is lowered by the blockade events. In this case, the blocker-induced bursts should last longer than the open periods of the channel in the absence of blocker (Colquhoun & Sigworth 1983). The experimental results (Table 5) disprove the application of this switching mode. An alternate model, which does satisfy the observations, consists of a

normal open/closed gating which is unaffected by the blocker, plus an extra "on/off" blocking mechanism in series. Thus, the entire switching pattern would be described by four states (open-on, open-off, closed-on, and closed-off). In these terms, the open/closed switch might well operate independently from the enzymatic reaction cycle for ion translocation, whereas the on/off switch is linked directly to the translocation cycle, as illustrated by Fig. 1*C*.

This work has been supported by the Deutsche Forschungsgemeinschaft.

## References


Bertl, A. 1989. Current-voltage relationships of a sodium-sensitive potassium channel in the tonoplast of *Chara corallina*. *J. Membrane Biol.* **109**:9–19

Bertl, A., Gradmann, D. 1987. Current-voltage relationships of potassium channels in the plasmalemma of *Acetabularia*. *J. Membrane Biol.* **99**:41–49

Colquhoun, D., Hawkes, A.G. 1982. On the stochastic properties of bursts of single ion channel openings and of clusters of bursts. *Phil. Trans. R. Soc. Lond. B* **300**:1–59

Colquhoun, D., Ogden, D.C. 1988. Activation of ion channels in the frog end-plate by high concentrations of acetylcholine. *J. Physiol.* **395**:131–159

Colquhoun, D., Sigworth, F.J. 1983. Fitting and statistical analysis of single-channel records. *In*: Single-Channel Recording. B. Sakmann and E. Neher editors. pp. 191–264. Plenum, New York

Cooper, K.E., Gates, P.Y., Eisenberg, R.S. 1988. Diffusion theory and discrete rate constants in ion permeation. *J. Membrane Biol.* **106**:95–105

Cooper, K.E., Jakobsson, E., Wolynes, O. 1985. The theory of ion transport through membrane channels. *Prog. Biophys. Molec. Biol.* **46**:51–96

Draber, S., Schultze, R., Hansen U.P. 1991. Patch-clamp studies on the anomalous mole fraction effect of the $K^+$ channel in cytoplasmic droplets of *Nitella:* an attempt to distinguish between a multi-ion single-file pore and an enzyme kinetic model with lazy state. *J. Membrane Biol.* **123**:183–190

Eisenman, G. 1962. Cation selective glass electrodes and their mode of operation. *Biophys. J.* **2**:259–323

Eyring, H., Lumry, R., Woodsbury J.W. 1949. Some applications of modern rate theory to physiological systems. *Record Chem. Prog.* **10**:100–114

Fisahn, J., Hansen, U.P., Gradmann, D. 1986. Determination of charge, stoichiometry and reaction-constants from IV-curve studies on a $K^+$-transporter in *Nitella*. *J. Membrane Biol.* **94**:245–252

FitzHugh, R. 1983. Statistical properties of the asymmetric random telegraph signal, with applications to single-channel analysis. *Math. Biosci.* **64**:75–89

Gagne, S., Plamondon, P.R. 1983. Tip potential of open tip glass microelectrodes: Theoretical and experimental studies. *J. Physiol. Pharmacol.* **61**:857–869

Gradmann, D., Klieber, H.G., Hansen, U.P. 1987. Reaction kinetic parameters for ion transport from steady state current-voltage curves. *Biophys. J.* **53**:287–292

Hamill, O.P., Marty, A., Neher, E., Sakmann, B., Sigworth, F.J. 1981. Improved patch-clamp techniques for high-resolution current recording from cells and cell-free membrane patches. *Pfluegers Arch.* **391**:85–100

Heinemann, S.H., Sigworth, F.J. 1991. Open channel noise VI. Analysis of amplitude histograms to determine rapid kinetic parameters. *Biophys. J.* **60**:577–587

Hille, B. 1984. Ionic Channels of Excitable Membranes. Sinauer, Sunderland, MA

Hille, B., Schwarz, W. 1978. Potassium channels as multi-ion single-file pores. *J. Gen. Physiol.* **72**:409–442

Läuger, P. 1980. Kinetic properties of ion carriers and channels. *J. Membrane Biol.* **57**:163–178

Laver, D.R. 1990. Coupling of $K^+$-gating and permeation with $Ca^+$ block in the $Ca^{2+}$-activated $K^+$ channel in *Chara australis*. *J. Membrane Biol.* **118**:55–67

Laver, D.R., Fairley, K.A., Walker, N.A. 1989. Ion permeation in a $K^+$ channel in *Chara australis:* direct evidence for diffusion limitation of ion flow in a maxi-K channel. *J. Membrane Biol.* **108**:153–164

Laver, D.R., Walker, N.A. 1987. Steady-state voltage dependent gating and conduction kinetics of single $K^+$ channels in the membrane of cytoplasmic drops of *Chara australis*. *J. Membrane Biol.* **100**:31–42

Laver, D.R., Walker, N.A. 1991. Activation by $Ca^{2+}$ and block by divalent ions of the $K^+$ channel in the membrane of cytoplasmic drops from *Chara australis*. *J. Membrane Biol.* **120**:131–139

Levitt, D.G. 1986. Interpretation of biological ion channel flux data—reaction rate versus continuum theory. *Annu. Rev. Biophys. Chem.* **15**:29–57

Lühring, H. 1986. Recording of single $H^+$ channels in the membrane of cytoplasmic drops of *Chara australis*. *Protoplasma* **133**:19–27

Mohan, M.S., Bates R.G. 1975. Calibration of ion-selective electrodes for use in biological fluids. *Clin. Chem.* **21**:864–872

Quartararo, N., Barry, P.H., Gage P.W. 1987. Ion permeation through single channels activated by acetylcholine in denervated toad sartorius sceletal muscle fibers: Effects of alkali cations. *J. Membrane Biol.* **97**:137–159

Robinson, R.A., Stokes R.H. 1965. Electrolyte Solutions. Butterworth, London

Sachs, F. 1983. Automated analysis of single channel records. *In*: Single-Channel Recording, B. Sakmann and E. Neher editors. pp. 265–286. Plenum, New York

Sachs, F., Neil, J., Barkakati, N. 1982. The automated analysis of data from single ionic channels. *Pfluegers Arch.* **395**:331–340

Schroeder, J.I., Hedrich, R., Fernandez, J.M. 1984. Potassium selective single channels in guard cell protoplasts of *Vicia faba*. *Nature* **312**:361–362

Sine, S.M., Claudio, T., Sigworth, F.J. 1990. Activation of *Torpedo* acetylcholine receptors expressed in mouse fibroblasts. Single channel current kinetics reveal distinct agonist binding affinities. *J. Gen. Physiol.* **96**:395–437

Spalding, E.P., Slayman C.L., Goldsmith, M.H., Gradmann, D., Bertl, A. 1992. Ion channels in *Arabidopsis* plasma membrane: transport characteristics and involvement in light-induced voltage changes. *Plant Physiol.* **99**:96–102

Vivaudou, M.B., Siger, J.J., Walsh, J.V. 1986. An automated technique for analysis of current transitions in multilevel single-channel recordings. *Pfluegers Arch.* **407**:355–364

Woodhull, A.M. 1973. Ion blockage of sodium channels in nerve. *J. Gen. Physiol.* **61**:687–708

Yellen, G. 1984. Ionic permeation and blockade in $Ca^{2+}$-activated $K^+$ channels of bovine chromaffin cells. *J. Gen. Physiol.* **84**:158–186


Received 12 June 1992; revised 24 September 1992